Frontiers of Environmental Science & Engineering
2025, 19(5): 71 https://doi.org/10.1007/s11783-025-1991-x

RESEARCH ARTICLE

N-doped activated carbon promoting sulfur-containing VOC removal in three-dimension electrode system

Rui Luo[1], Shugen Liu ✉ [1,2], Senlin Tian[1,2], Chen Li[1], Ping Ning ✉ [1,2]

1. Faculty of Environmental Science and Engineering, Kunming University of Science and Technology, Kunming 650500, China
2. National Regional Engineering Research Center-NCW, Kunming 650500, China

HIGHLIGHTS

- The urea-modified AC enhanced S-VOCs purification in 3DES system.
- Particle electrode enhanced adsorption capacity and dielectric properties.
- PDS was efficiently activated by carbon-based material and electrochemistry.
- Radical and non-radical oxidation had significant contributions for S-VOC purification.

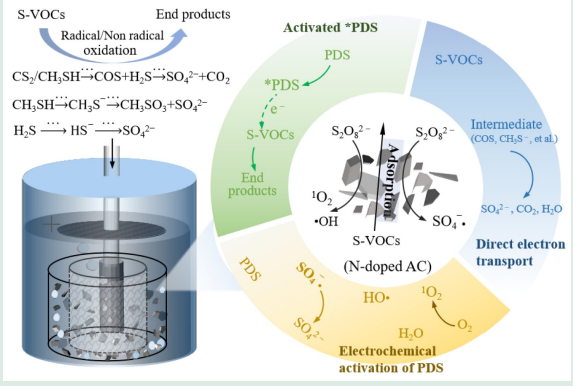

ABSTRACT: N-doped activated carbon (AC) was employed in a three-dimensional electrode system (3DES) to enhance the removal of sulfur-containing volatile organic compounds (S-VOC). The technical parameters for preparing N-doped AC were optimized based on CS_2 removal and COS accumulation, where the mass ratio of AC to urea was 1:1.0, and the activation temperature and heat-treatment time were 400 °C and 120 min, respectively. When the mixing S-VOC were purified under an operating voltage of 8 V and peroxydisulfate concentration of 0.15 mol/L, CS_2 removal in the 3DES system with N-doped AC reached 100% within 75 min, and was above 83% as purification time extended to 200 min. Additionally, the COS content in the outlet gas was usually undetectable within 120 min, and was lower than that in the other electrochemical systems. Modification of raw AC through urea impregnation and subsequent heat treatment significantly improved its surface structure and pore size distribution. Moreover, polar functional groups, such as C=O and pyridinic-N, increased noticeably, enhancing the S-VOC adsorption capacity and dielectric properties. Consequently, highly reactive substances were more efficiently activated in 3DES system with N-doped AC, and oxidizing species HO• and $^1O_2$ had important contributions to S-VOC purification compared to SO_4^{-}• radicals. A pathway was proposed to elucidate the transformation of sulfur-containing components, such as CH_3SH and CS_2. This study provides an efficient approach for S-VOC purification.

KEYWORDS: N-doped activated carbon, Sulfur-containing VOC, Three-dimensional electrode system, Electrochemical oxidation

✉ Corresponding authors. E-mails: bridgelsg@sina.com (S. Liu); Ningping58@sina.com (P. Ning)

Article history: Received 8 October 2024, Revised 1 February 2025, Accepted 5 March 2025, Available online 7 April 2025

1 Introduction

Sulfur-containing volatile organic compounds (S-VOC) are mainly derived from industrial processes such as oil refining, printing and dyeing, and chemical production, and are main contributors to severe environmental pollution, including fine particulate matter and ozone formation. Even low concentration of S-VOC may lead to a direct severe threat to materials and human health (Tian et al., 2023). Thus, the treatment of malodorous S-VOC, such as CH_3SH and CS_2, has become a pressing issue.

The main technologies for S-VOC removal include adsorption, photocatalysis, advanced oxidation, catalytic decomposition, and biodegradation (Lyu et al., 2020; Yang et al., 2020; Xiao et al., 2021; Yao et al., 2024). Catalytic decomposition is usually regarded as one of the most effective routes for S-VOC removal (Yang et al., 2020; Tian et al., 2023). Many functional materials, including activated carbon (AC), ZSM zeolites, and hydrotalcite-like compounds have been developed to facilitate S-VOC conversion (Zhao et al., 2018; Qu et al., 2022). Several studies have focused on decreasing reaction temperatures and extending the service life of catalyst using different preparation methods or modification treatments (He et al., 2017; 2019; Jin et al., 2021). Although rare and precious metal catalysts have been developed to improve performance, avoiding the generation of toxic and harmful intermediate components such as COS and H_2S is difficult because sulfur-containing substances such as CH_3SH and CS_2 are easily hydrolyzed during the catalytic process. To address this, advanced oxidation is required for the complete conversion of S-VOC.

Electrochemical oxidation has recently gained popularity for its strong adaptability and high efficiency. A novel approach has been developed to remove S-VOC from the air stream (Chen et al., 2019), where CS_2 is absorbed in water and then broken down by an electrochemical reaction at a RuO_2 electrode loaded with titanium. Additionally, *in situ* ferrate (VI) generation in a wet oxidation system facilitated CH_3SH conversion under optimized conditions of 6 mol/L NaOH and a current density of 14.06 mA/cm^2 (Ding et al., 2012). Since conventional electrochemical systems usually suffer from low mass transfer and current efficiency (Zhang et al., 2013), a three-dimensional electrode system (3DES) has been constructed to improve the degradation of atrazine (Li et al., 2019), which is also used to activate peroxydisulfate (PDS) for purifying sulfur-containing malodourous gases (Luo et al., 2024). In 3DES, AC or carbon fiber tubes are widely used as particle electrodes, and redox reactions take place in small particles, effectively increasing the surface area of the electrode and boosting current efficiency (Wang et al., 2024). Numerous experiments have confirmed that nano-carbon materials, such as reduced graphene oxide, porous carbon, and carbon nanotube, perform well in pollutant decomposition. However, their applications are limited owing to their high cost and complicated preparation processes. Some researchers have sought to dope carbon matrices with heteroatoms such as S, N, or P (Wang et al., 2020) to enhance pollutants decomposition. For instance, N doping not only modifies the properties of the AC surface and charge transport but also forms more reactive sites, such as N-pyridinic, N-pyrrolic and pyridinone nitrogen moieties. Consequently, the modified carbon materials promote the selective catalytic reduction of NO_x (Li et al., 2023).

Focusing on the efficient purification of S-VOC, this study constructed a 3DES system with N-doped AC to activate PDS. Based on preliminary experiments, urea was selected as the chemical reagent to modify the carbon material. Key factors, including the mass ratio of AC to urea, activation temperature, and heat-treatment time, were optimized, and the effects of technical parameters in the electrochemical system on S-VOC removal were analyzed. Finally, a conversion pathway was proposed to elucidate the transformation of sulfur-containing components. These results provide important theoretical references and technical support for the purification of S-VOC.

2 Materials and methods

2.1 Startup of 3DES system

Batch experiments were conducted in a cylindrical 3DES apparatus, as reported in our previous study (Luo et al., 2024). The effective volume of the apparatus was 1.4 L. The anode and the cathode consisted of platinum-plated titanium mesh and titanium sheet, respectively, while the particle electrode was a circular plastic cavity filled with 5 g of granular AC.

CS_2, CH_3SH, H_2S, and N_2 were mixed in specific proportions, with the concentrations of three sulfur-containing components being 50, 65, and 70 mg/m^3, respectively. The simulated S-VOC was supplied to the electrochemical device at a flow rate of 4.8 L/h. The gaseous S-VOC were purified by electro-activated PDS in the 3DES reactor. All experiments were performed in duplicate to ensure the stability and repeatability of the results.

2.2 Preparation of N-doped AC

The raw AC was treated by boiling in water for 15 min, washed twice with deionized water, and then dried at 50 °C for 12 h. The resulting carbon material was mixed with chemical reagent urea. The solid mixture was immersed in deionized water at 50 °C for 24 h, with a mixture-to-water ratio of 1:2 (w:v). Afterward, the impregnating solution was discarded. The resulting carbon material was activated at a specific temperature for a specific duration, with nitrogen as the protective gas at a flow rate of 5.0 L/h. The obtained product was designated as N-doped AC. A control check of activated carbon, that is, CK-AC, was prepared using the same procedure but without the addition of urea.

Based on the preliminary experiments, the key factors for N-doped AC preparation were as follows: mass ratio of AC to urea was 1:0.5, 1:1.0, and 1:1.5, the activation temperature was 200, 400, and 600 °C, and the heat-treatment time was 60, 120, and 180 min. The effects of N-doped AC on CS_2 removal and COS accumulation were tested under the conditions of a PDS solution of 0.15 mol/L, initial pH 8.0, direct current (DC) voltage of 8 V, in which the initial conductivity of the electrolyte was 20 mS/cm.

2.3 Comparative experiments for S-VOC removal

Comparative experiments were conducted to optimize the operating voltage and PDS concentration in the 3DES process. Considering the components of S-VOC are complex, NH_3 was simultaneously added to the simulated S-VOC, and its concentration was 120 mg/m^3. The technical parameters for N-doped AC preparation were mass ratio of 1:1.0, activation temperature of 400 °C, and heat-treatment time of 120 min, the other operating conditions not mentioned here were the same as above.

2.4 Analysis and characterization

CS_2, CH_3SH, COS, and H_2S were determined using a gas chromatograph (GC-9790 Plus, Fuli Instruments, China) equipped with flame a photometric detector (Chen et al., 2019; Tian et al., 2023). The $S_2O_8^{2-}$ concentration was measured via a modified iodometric method (Liang et al., 2008) using a UV–Vis spectrophotometer (DR 6000, HACH, USA) at 352 nm. The resulting hydroxyl radical (HO•), sulfate radical (SO_4^{-}•), and singlet oxygen ($^1O_2$) were captured by 5, 5-dimenthy-l-pyrrolin-N-oxide (DMPO) and 4-oxo-2,2,6,6-tetramethylpiperidine (TEMP), respectively. Electron paramagnetic resonance (EPR) spectra were obtained using a Bruker EPR spectrometer (A300, Germany) (Sun et al., 2020).

For the carbon-based material, the surface compositions and combination states of the elements were analyzed using X-ray photoelectron spectroscopy (XPS, K-Alpha, Thermo Fisher Scientific, USA). The functional groups were observed using a Fourier transform infrared (FT-IR) spectrometer (Nicolet iS20, Thermo Fisher Scientific, USA), and the specific surface area and pore size distribution were quantified using the ASAP 2460 (Micromeritics Corp., USA) BET analyzer. Cyclic voltammetry (CV) and linear sweep voltammetry (LSV) curves were obtained using an electrochemical workstation (CHI660E, Shanghai Chenhua Co., Ltd., China) with a three-electrode system.

3 Results and discussion

3.1 Preparation of N-doped AC

The N-doped AC was prepared under specific conditions and used in the 3DES system to remove S-VOC. Since the purification efficacy for CS_2 is relatively poor and COS is a potential intermediate in S-VOC conversion (He et al., 2019; Luo et al., 2024), the concentrations of CS_2 and COS were regularly measured. The variations in CS_2 removal and COS accumulation are shown in Fig. 1. When the mass ratio of AC to urea was 1:0.5 or 1:1.5, the N-doped AC showed poor purification of S-VOC, the CS_2 removal in the 3DES was less than 83% at 45 min, and the COS content in the outlet gas was up to 3.9 mg/m^3 at the same time (Figs. 1(a) and 1(b)). In comparison, the optimal mass ratio of AC to urea was 1:1.0, where the CS_2 removal efficiency in the 3DES system with N-doped AC was maintained 100% within 75 min, and it was also higher than 83% when the gas purification time was extended to 200 min. Meanwhile, the COS concentration was too low to be detected within 120 min. Thereafter, its content in the outlet gas did not exceed 1.7 mg/m^3. Similarly, the optimized technical parameters for the N-doped AC, including an activation temperature of 400 °C and a heat-treatment time of 120 min, were derived based on the CS_2 removal and COS accumulation observed in the electrochemical system (Figs. 1(c)–1(f)).

Compared to the raw carbon material, the N-doped AC enhanced the efficacy of CS_2 removal in the 3DES, and the accumulated intermediate COS was relatively low (Figs. 1(a) and 1(b)), indicating that the carbon-based material via urea modification facilitated S-VOC

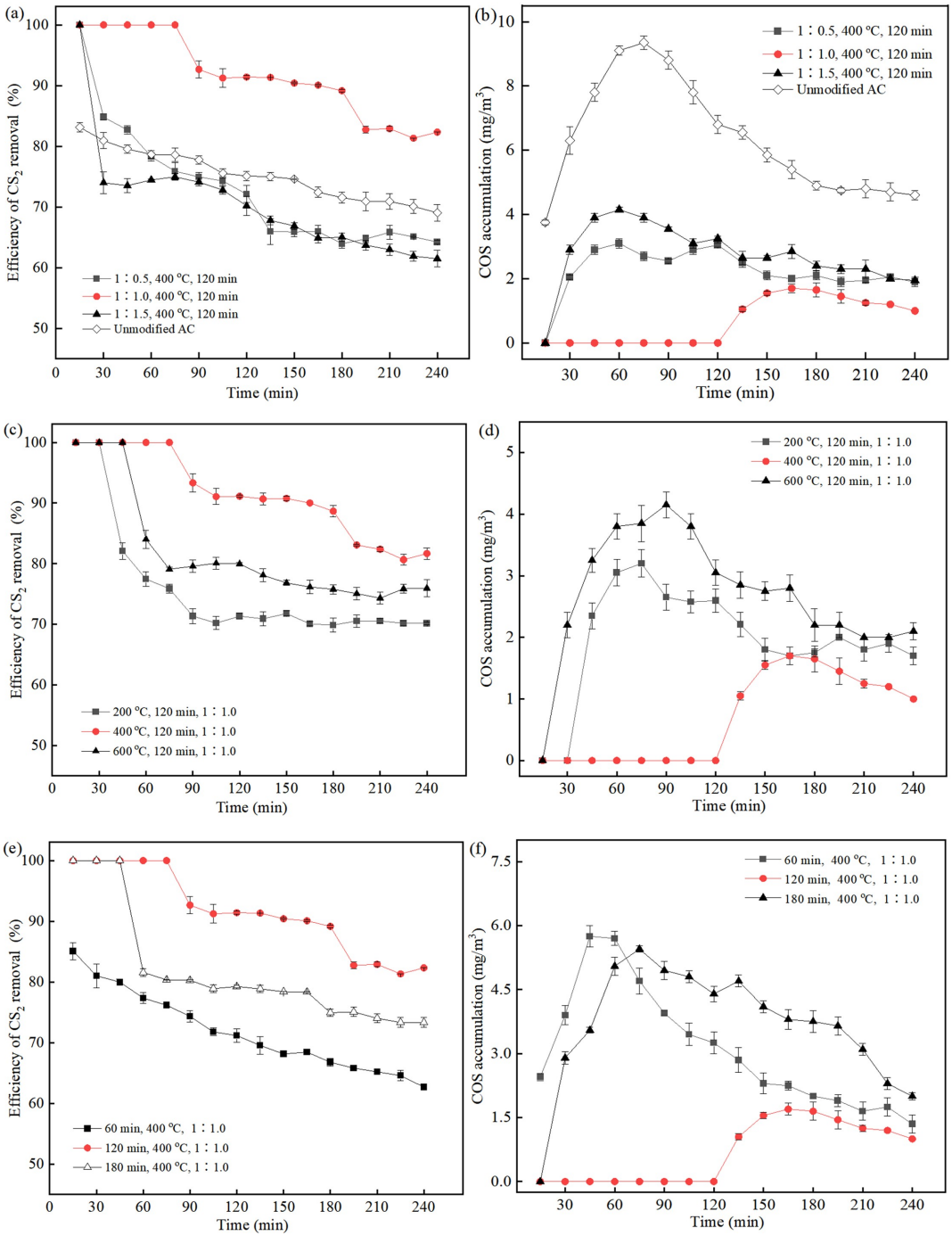

Fig. 1 Variations of the CS_2 removal and COS accumulation in electrochemical system with N-doped AC. (a)–(b) Mass ratio of AC to urea, 1:0.5/1:1.0/1:1.5, (c)–(d) activation temperature, 200/400/600 °C, (e)–(f) heat-treatment time, 60/120/180 min.

purification. Doping can change the physicochemical properties of carbon material by forming specific functional groups or changing the specific surface area and pore size distribution (Yang et al., 2016; Wang et al., 2020; Hong and Jo, 2024), which provide favorable conditions for the conversion of sulfur-containing substances in the 3DES. As the mass ratio of AC to urea increased to 1:1.5 or the activation temperature reached 600 °C, the modification of the carbon material maintained a relatively weak CS_2 removal, indicating that high urea content or high activation temperature is not beneficial for improving

the performance of carbon material in the 3DES. This outcome was likely due to excessive etching of the carbon skeleton and the rapid collapse of microporous channel. Additionally, maintaining a suitable heat-treatment time for the N-doped AC was crucial, as it helped to open the micropores open and generate more oxygen- and nitrogen-containing functional groups on the AC surface (Yang et al., 2016; Li et al., 2023). Thus, the electrochemical system with N-doped AC derived from a 120-min heat-treatment showed superior CS_2 removal and lower COS accumulation than those in the other two 3DES systems (Figs. 1(e) and 1(f)).

3.2 Effects of electrochemical parameters on S-VOC removal

3.2.1 Operating voltage

The effects of the operating voltage on S-VOC removal were investigated in this study. As shown in Fig. 2, the purification efficiencies for CH_3SH, H_2S, and NH_3 in the three electrochemical systems were approximately 100% within 240 min (Fig. 2(a)). However, the CS_2 removal and COS accumulation were significant different at different voltage levels (Figs. 2(b) and 2(c)). The system with a DC voltage of 8 V maintained efficient performance for S-VOC purification. CS_2 removal reached 100% within 75 min, and then gradually decreased, with an average CS_2 removal of 87.4% during the period of 90–240 min. On the other hand, COS was too low to be detected before 120 min, and its concentration in the outlet gas maintained below 2.0 mg/m^3. The average value of COS accumulation from 135 to 240 min was only 1.45 mg/m^3. When the DC voltage in the 3DES was changed to 6 or 10 V, the electrochemical system exhibited relatively lower CS_2 removal and higher COS accumulation. For the system with a DC voltage of 10 V, the CS_2 removal showed a rapid decrease, and intermediate COS in the outlet gas could be detected when the treatment time was longer

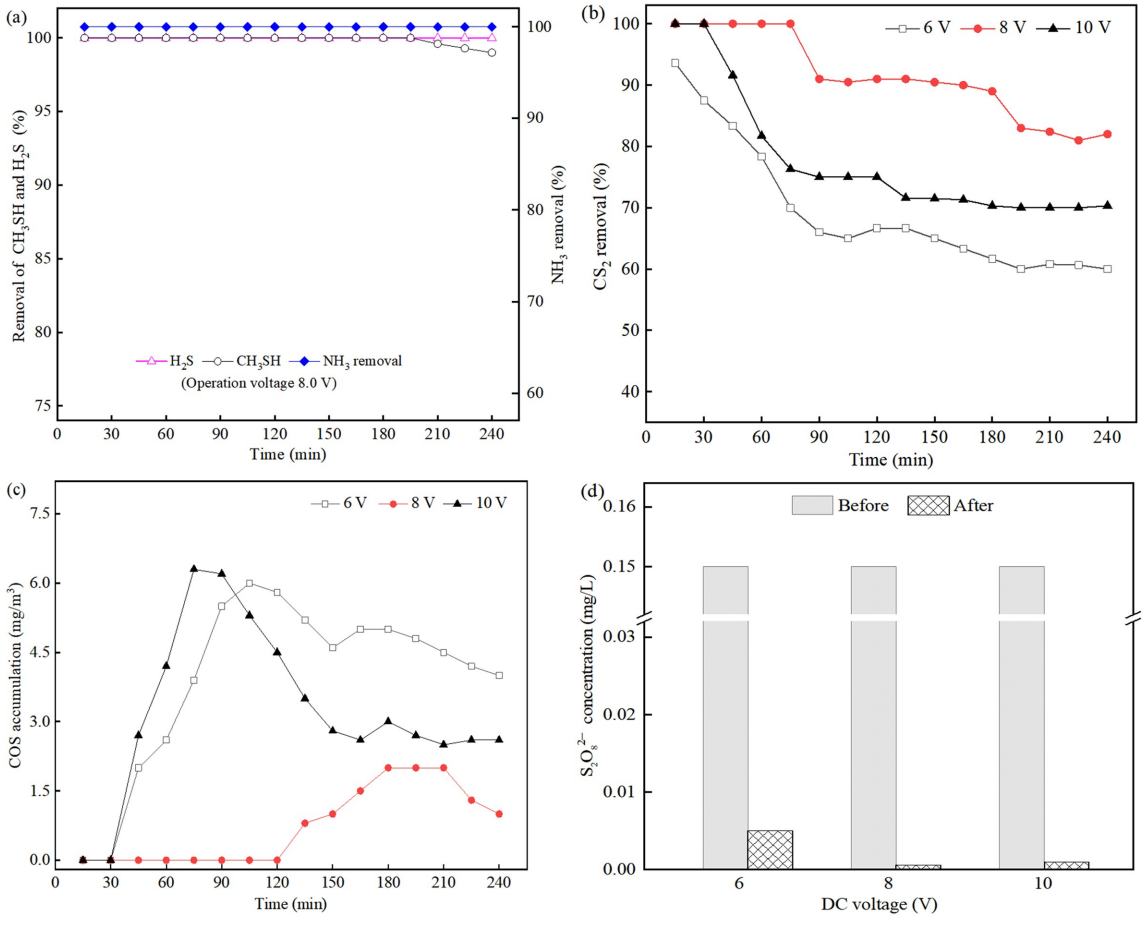

Fig. 2 S-VOC purification at different DC voltage. (a) Removal efficacy for CH_3SH, H_2S, and NH_3, (b) CS_2 removal, (c) COS accumulation, (d) $S_2O_8^{2-}$ concentration in solution (CS_2 50 mg/m^3, CH_3SH 65 mg/m^3, H_2S 70 mg/m^3, NH_3 120 mg/m^3, PDS 0.15 mol/L, initial pH 8.0, operating temperature 293 K, and inlet gas flow rate 4.8 L/h).

than 30 min. Therefore, a DC voltage of 8 V was deemed suitable for S-VOC purification.

For the 3DES system with N-doped AC, the oxidation capacity tended to become stronger with the increase in DC voltage due to the activation of $S_2O_8^{2-}$ ions, and $S_2O_8^{2-}$ concentration at 240 min decreased markedly (Fig. 2 (d)) in a manner relating to the consumption of the oxidizing agent. Based on the chemical reaction Eqs. (1)–(3), increasing voltage enhances the polarization of electrode potential (Jing et al., 2022), which accelerates the decomposition of PDS. This results in the efficient removal of pollutants by highly active substances, such as HO• and SO_4^{-}•. Consequently, the electrochemical system with a DC voltage of 8 V maintained a relatively high CS_2 removal and low COS accumulation (Figs. 2(a)–2(c)). However, a higher current intensity inevitably increases the short-circuit and bypass currents and intensifies side reactions such as oxygen evolution and hydrogen evolution (Jing et al., 2022; Luo et al., 2024). Therefore, a high voltage of 10 V is not conducive to S-VOC purification.

$$O_2 + 2H^+ + 2e^- \rightarrow H_2O_2 \quad (1)$$

$$H_2O \rightarrow HO\cdot + H^+ + e^- \quad (2)$$

$$S_2O_8^{2-} + e^- \rightarrow SO_4^{\cdot-} + SO_4^{2-} \quad (3)$$

3.2.2 PDS concentration

PDS acts as a precursor for highly active substances in an electrochemical system (Zhang et al., 2013; Li et al., 2019). Therefore, comparative experiments were conducted at different PDS concentrations. As shown in Fig. 3, the efficacy of S-VOC purification significantly improved as the initial PDS concentration increased from 0.10 to 0.15 mol/L. For the electrochemical

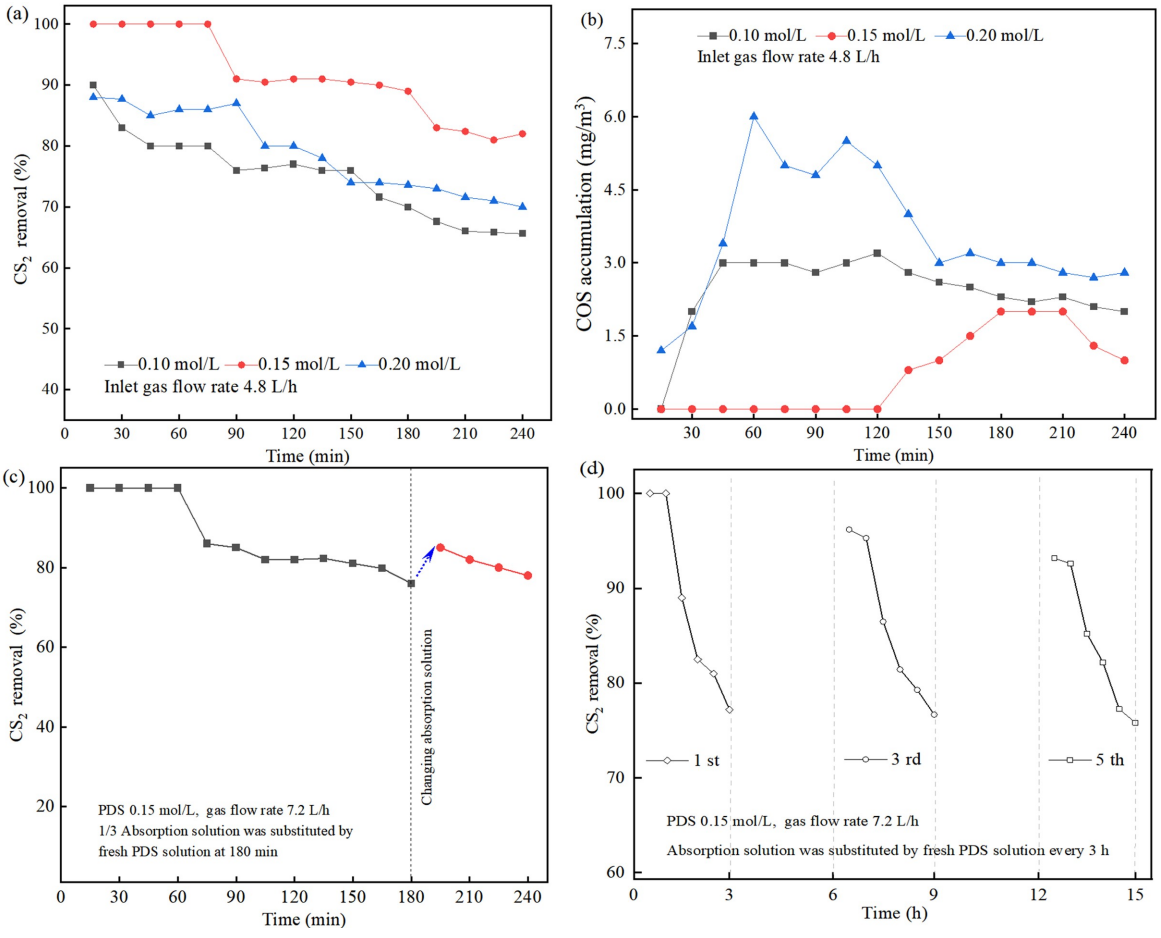

Fig. 3 S-VOC purification at different PDS concentrations. (a) CS_2 removal, (b) COS concentration, (c) CS_2 removal after intermittent addition of PDS, (d) CS_2 removal under cyclic test condition (DC voltage 8 V, and the other conditions were the same as that in Fig. 2).

system with an initial PDS concentration of 0.15 mol/L, CS_2 removal reached 100% before 75 min, and showed a moderate decrease thereafter. However, the purification efficiency of S-VOC tended to be worse as the PDS concentration increased to 0.20 mol/L, indicating that excessive PDS was unfavorable to the S-VOC removal. The finding was also consistent with the research result that excessive PDS in absorption solution causes the scavenging of the SO_4^{-}• radical (Cui et al., 2017). The electrochemical system with PDS concentration of 0.15 mol/L obtained relatively stronger oxidation for sulfur-containing intermediates. COS content in the outlet gas was usually undetectable within 120 min, and the highest value was less than 2.0 mg/m^3 even during the period of 120–240 min, substantially lower than those in the other two systems.

As PDS is added to an electrochemical system, the SO_4^{-}• radical is produced by electrochemical activation (Luo et al., 2024), facilitating the S-VOC removal and conversion of sulfur-containing intermediates. With the continuous depletion of the SO_4^{-}• radical derived from S-VOC oxidation, a certain amount of PDS was converted to sulfate ions, resulting in the decline of S-VOC removal and moderate COS accumulation (Figs. 3(a) and 3(b)). When one-third of the absorption solution was discarded at 180 min and an equal volume of PDS solution with an initial concentration of 0.15 mol/L was subsequently added to the reaction system, CS_2 removal was enhanced from 76.0% at 180 min to 85% at 195 min (Fig. 3(c)). Furthermore, cycling performance of the 3DES system indicated that CS_2 removal exhibited a moderate decline, whereas for the fifth cycle of S-VOC purification, CS_2 removal decreased from 91.3% at 13 h to 79.0% at 14 h (Fig. 3(d)). It can be concluded that maintaining an appropriate PDS concentration is very important for S-VOC purification, and the performance of the carbon material decreases after long-term operation.

3.3 Characteristics of S-VOC purification

3.3.1 Properties of carbon-based materials

To investigated the effects of carbon-based material on S-VOC purification, adsorption tests were conducted in a 3DES device without DC current or PDS addition. As shown in Fig. 4(a), the adsorption curves for raw AC, CK-AC, and N-doped AC showed similar trend. However, the maximum CS_2 adsorption capacity of N-doped AC was 0.126 mg/g, which was three times that of raw AC. The adsorption curve for N-doped AC showed a rapid increase within 200 min, significantly higher than that of the raw AC, indicating that the adsorption rate of S-VOC on the N-doped AC was significantly enhanced. Consequently, gaseous sulfur-containing components can remain in the absorption solution for a long time, providing a favorable external environment for the subsequent oxidation of S-VOC.

Carbon-based materials, including raw AC, CK-AC, and N-doped AC, were used to investigate the variations in surface properties. As shown in Fig. (b), the peaks at 2850 and 2920 cm^{-1} were attributed to the symmetric and antisymmetric stretching vibrations of alkyl-CH_2 groups, while the peaks at 1641 and 1097 cm^{-1} were assigned to the stretching vibrations of C=O and C–O bonds, respectively. Additionally, the peak at 1437 cm^{-1} was related to the C–N bending vibration (Yang et al., 2016; Luo et al., 2024). The FT-IR spectra of the samples revealed that functional groups, such as alkyl-CH_2, C–N and C–O bonds, were significantly enhanced after AC modification. The elemental compositions of raw AC and N-doped AC were compared using XPS analysis. The binding energies of 285 and 400 eV were attributed to C1s and N1s respectively. The C1s spectra showed peaks at 284.5, 285.2, 286.3, and 289 eV (Fig. 4(c)), which were assigned to C–C/C=C, C–O/C–N, C=O, and COOH groups, respectively (Hong and Jo, 2024). For N-doped AC, the C–C/C=C content was 64.9%, while the C–O/C–N and C=O contents reached 26.4%, which were obviously higher than the 19.6% observed in the raw AC, indicating that AC modification with urea moderately changed the surface functional groups of the carbon material. The C=O functional group on the AC surface is the major reaction site for PDS activation to produce $^1O_2$ (Zhu et al., 2018), and is abundant in N-doped AC, thereby contributing to the formation of highly reactive substances. The N1s spectra were partitioned into three peaks at approximately 398.4, 399, and 400 eV (Fig. 4(d)), corresponding to pyridinic N, amine-N/amide-N, pyrrolic N (Wang et al., 2022), with proportions of 28.3%, 49.1%, 22.6%, respectively. Among the three types of C–N functional groups, the negatively charged pyridinic N groups have a relatively high dipole moment, enhancing the wettability of the electrode and providing abundant active sites to promote redox reaction (Ghosh et al., 2020).

According to the guidelines stipulated by the International Union of Pure and Applied Chemistry, AC has well-developed micropores, and its adsorption equilibrium is usually described by a type I adsorption isotherm. For the N-doped AC derived through urea modification, the specific surface area increased to 1168 m^2/g, while the total pore volume and micropore volume for 1 g carbon material were 0.73 and 0.34 cm^3, respectively. Additionally, the average pore diameter was elevated to 2.5 nm (Table 1), indicating that the

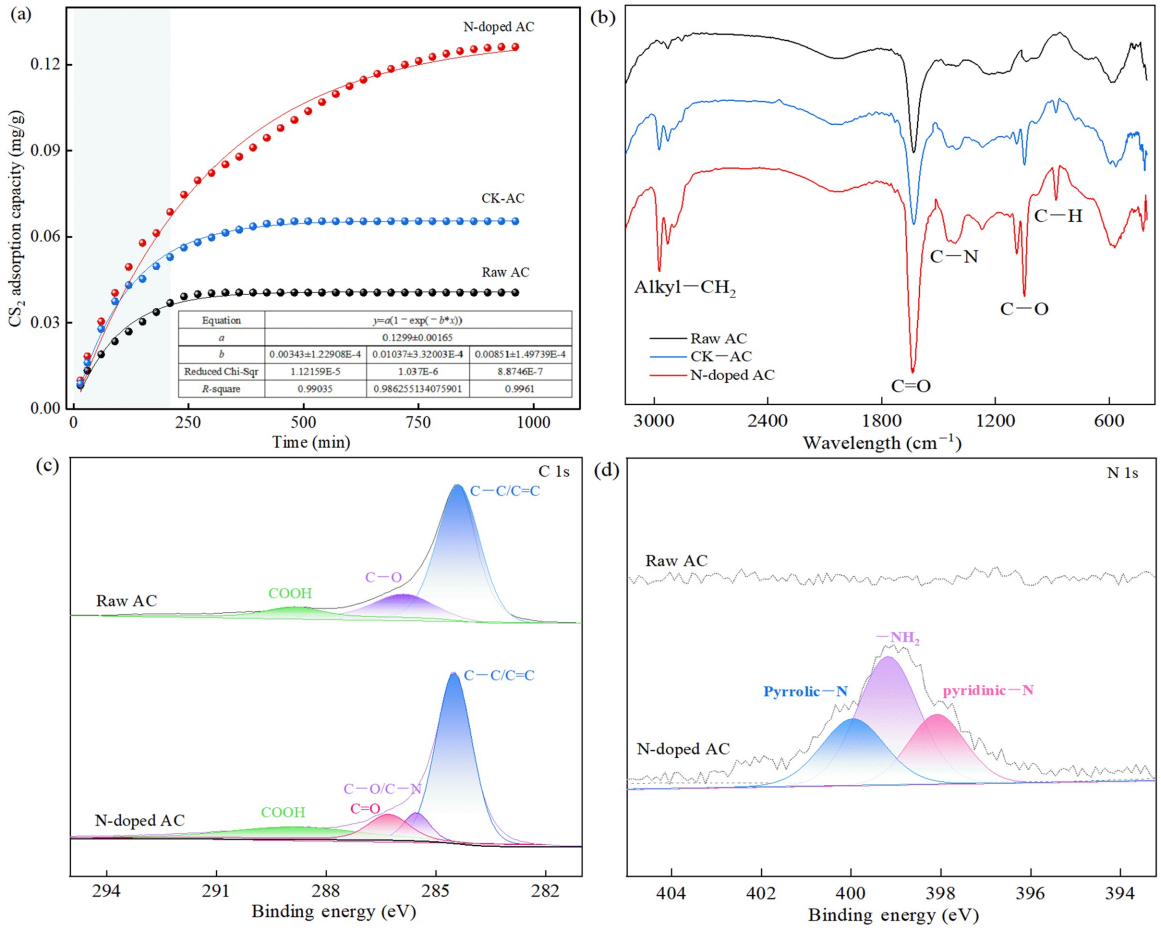

Fig. 4 Adsorption properties of carbon materials. (a) CS_2 adsorption capacity, (b) FT-IR spectra, (c) C1s XPS spectra, (d) N1s XPS spectra.

percentage of mesopores for N-doped AC moderately increased and the adsorption equilibrium tended to be type-IV adsorption isotherm. When urea was used to modify the properties of the carbon material, the surface structure and pore size distribution improved significantly, which was beneficial for enhancing the performance of the electrochemical system.

3.3.2 Reactive substances affecting purification process

Scavengers were introduced into the electrochemical system to elucidate the effects of reactive substances on S-VOC purification. Methyl alcohol (MeOH) was used to quench SO_4^{-}• and HO•, tert-butyl alcohol (TBA) was used to quench HO•, and furfuryl alcohol (FFA) was regarded as a scavenger to analyze the effect of $^1O_2$ on substrate decomposition (Huang et al., 2014; Feng et al., 2017). In this study, the carbon-based materials, including raw AC, CK-AC, and N-doped AC were used as three-dimensional particle electrodes, and three kinds of scavengers, i.e., MeOH, TBA, and FFA, were respectively added to the 3DES systems, with the solution concentration of 50 mmol/L. Operational conditions included a CS_2 content of 60 mg/m^3, DC voltage of 8 V, and inlet gas flow rate of 6.0 L/h. Other parameters not mentioned here were the same as those in Fig. 2. For all three electrochemical systems, the CS_2 removals exhibited a decreasing tendency after adding the scavenger (Figs. 5(a) and 5(b)), revealing that the highly reactive substances such as SO_4^{-}•, HO•, and $^1O_2$ existing in 3DES play significant role in S-VOC purification. Compared with the electrochemical systems with raw AC or CK-AC, the efficacy of CS_2 removal in the N-doped AC system showed a significant increase, and the curve exhibited a decline after the reactive substances were quenched by the scavenger (Fig. 5(b)). When FFA was added to the 3DES systems containing raw AC or N-doped AC, the average reductions in CS_2 removal during 30–60 min (Figs. 5(a) and 5(b)) were 24.3% and 46.6%,

Table 1 Variations of specific surface area and pore size distribution of adsorbent materials

Type	S_{BET}[1] (m^2/g)	S_{mic}[2] (m^2/g)	S_{ext}[3] (m^2/g)	V_{tot}[4] (cm^3/g)	V_{mic}[5] (cm^3/g)	D_p[6] (nm)
Raw AC	881	673	218	0.50	0.27	2.15
CK-AC	910	719	198	0.49	0.28	2.28
N-doped AC	1168	836	332	0.73	0.34	2.5

Remark: 1. BET surface area; 2. micropore area; 3. external surface area; 4. total pore volume; 5. micropore volume; 6. average pore diameter.

respectively. Based on the reduction in CS_2 removal after adding the scavenger, it can be inferred that the order of highly reactive substances degrading S-VOC in the raw-AC 3DES system was HO• > $^1O_2$ > SO_4^{-}•. However, after the carbon material was modified with urea, S-VOC purification in the electrochemical system was performed in the following order: $^1O_2$ > HO• > SO_4^{-}•. The treatment of N-doped AC enabled non-free radicals, particularly $^1O_2$, to play a significant role in CS_2 removal. Additionally, the reduction in CS_2 removal in the electrochemical systems increased with extended purification time after the addition of scavengers (Figs. 5(a) and 5(b)). This suggests that another pathway plays an important role in S-VOC decomposition in addition to the oxidation of SO_4^{-}•, HO•, and $^1O_2$.

In this study, DMPO and TEMP were used to investigate variations in free and non-free radicals. As shown in Figs. 5(c) and 5(d), the concentrations of HO •, SO_4^{-}•, and $^1O_2$ in the three 3DES systems moderately increased as the time extended from 5 to 20 min, and the EPR intensities of $^1O_2$ and HO• were significantly higher than those of SO_4^{-}•. Furthermore, the signals of HO• and $^1O_2$ in the N-doped system were

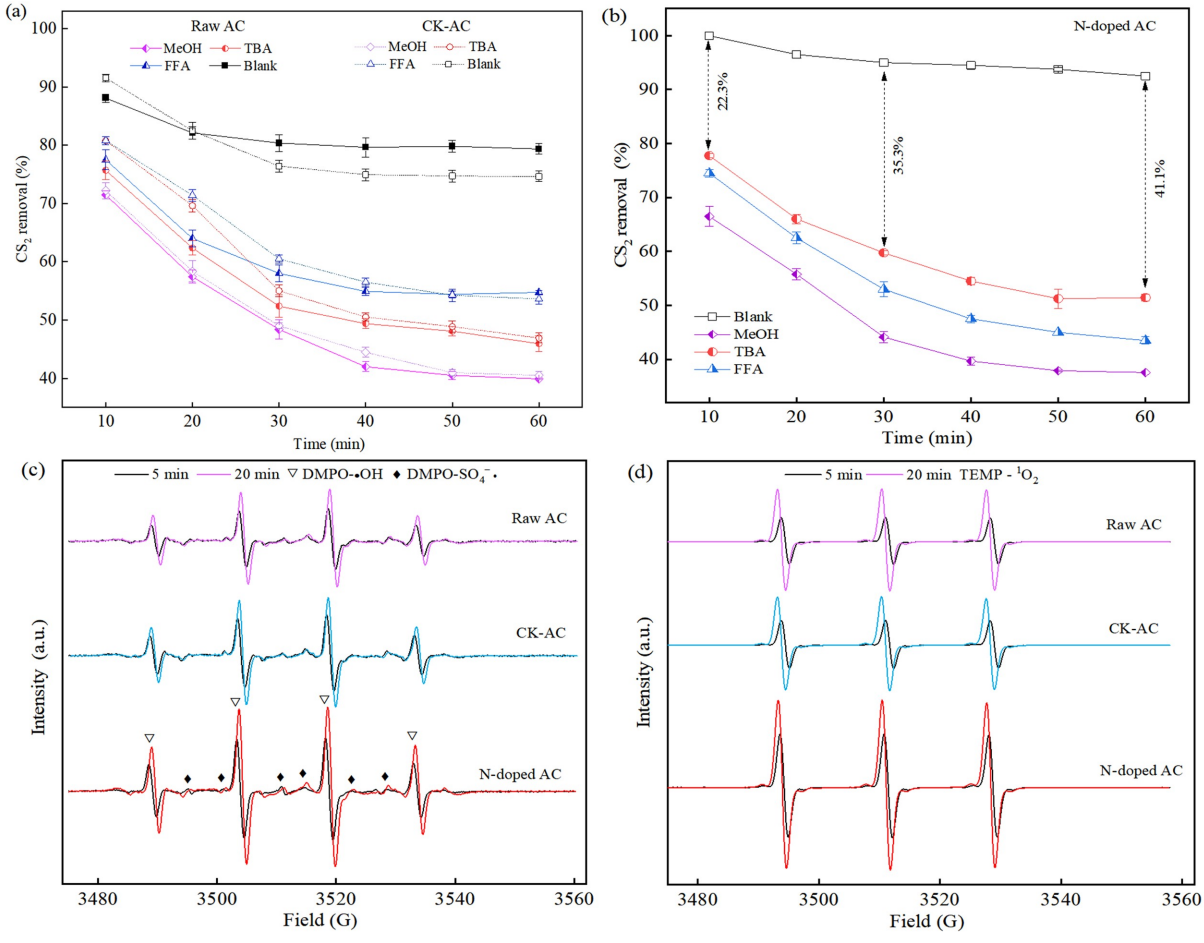

Fig. 5 Variations in CS_2 removal and reactive substance. (a) CS_2 removal in the raw AC system, (b) CS_2 removal in the N-doped AC system, (c) EPR spectra of SO_4^{-}• and HO•, (d) EPR spectra of TEMP-$^1O_2$.

substantially stronger as compared to those in the raw AC system. This result is also accordance with the fact that PDS can be activated by N-doped AC and electrolysis to produce highly reactive substances including HO•, $^1O_2$, and SO_4^{-}• (Liu et al., 2019; Zheng et al., 2021).

3.3.3 Electrochemical properties of N-doped AC

Electrochemical properties of the carbon-based materials were analyzed by cyclic voltammograms (Figs. 6(a)–6(c)), where the sweep rate was 0.04–0.10 V/s, the electrolytes were 50 mmol/L $K_4Fe(CN)_6$ and 0.5 mol/L Na_2SO_4. The redox reaction of $K_3Fe(CN)_6/K_4Fe(CN)_6$ produces two sharp peaks, and the anodic and cathodic current peaks become stronger with increasing sweep rates. Simultaneously, there is a good linear relationship between the oxidation peak current (I_p) and the square root of the scan rate ($v^{1/2}$), according to the following equation (Li et al., 2016).

$$I_P = (2.69\times10^5)\times n^{2/3}\times A\times D_R^{1/2}\times C_R\times v^{1/2} \quad (4)$$

where n is the number of transferred electrons, A is the electrochemically active surface area (ECSA) (cm^2), D_R is the diffusion coefficient of the reduced species (cm^2/s), C_R is the bulk reduced species concentration (mmol/L), and v is the scan rate (mV/s). The above-mentioned equation can be simplified as following: $I_p = k\,v^{1/2}$, here k is a coefficient relevant only to A and D_R as n and C_R were constant in this study. As shown in the insets of Figs. 6(a) and 6(b), the slopes of the linear relationship between I_p and $v^{1/2}$ –namely, the values of k– were obtained via linear fitting of the plots. For raw AC and N-doped AC, the coefficient values in the electrochemical systems were 0.0058 and 0.0122, respectively, indicating that the N-doped AC had a better mass transfer performance. Nitrogen and carbon atoms have similar atomic radii, and carbon atoms in

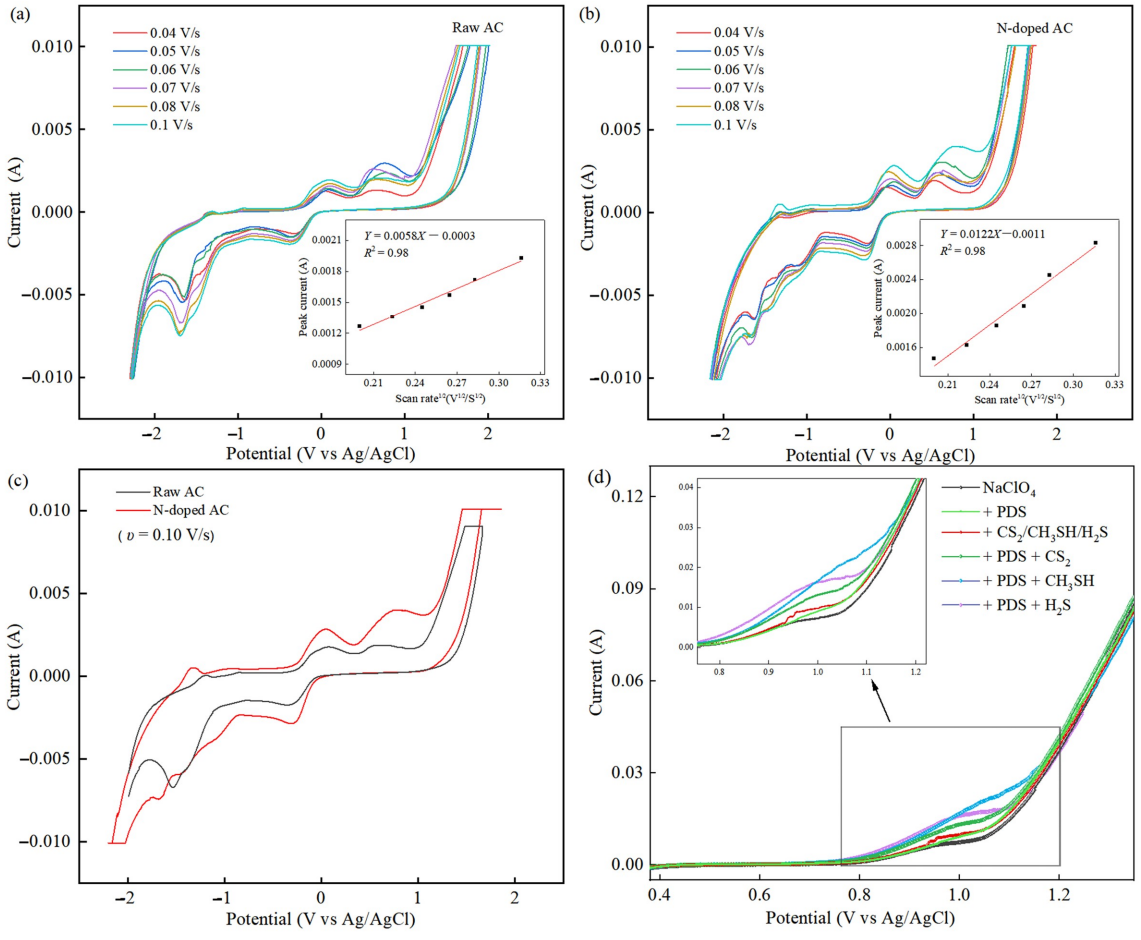

Fig. 6 Cyclic voltammograms of electro-chemical systems. (a) CV curves in the raw AC system, (b) CV curves in the N-doped AC system, (c) the difference in CV curves derived from the raw and N-doped AC systems, (d) linear sweep voltammetry.

raw AC can be replaced by nitrogen atoms more conveniently during the modification process. The electronegativity of nitrogen and changes in the electron density generally result in the formation of electron-defective sites in the lattice structure of the carbon material (Erlind et al., 2023), which can enhance the electron transfer ability and improve the electrocatalytic performance. Thus, the efficacy of S-VOC purification improved significantly after raw AC was modified by urea impregnation and subsequent heat treatment.

The redox behavior and oxygen evolution potential (OEP) during electrode oxidation were evaluated by LSV curves in the three-electrode system with 0.5 mol/L $NaClO_4$ electrolyte solution (Fig. 6(d)). The OEP of the raw AC system was 0.756 V, which increased to 0.860 V for the N-doped AC system. The N-doped AC electrode exhibited a relatively high OEP, which could reduce the side reactions of water electrolysis and enhance the efficiency of electrochemical oxidation. In addition, the current at the working electrode increased significantly as the sulfur-containing inlet gas was introduced into PDS solution, and the oxidation peaks were much stronger than those in the blank control without the addition of PDS. The findings revealed synergistic effects between the PDS solution and the electrode in the electrochemical system.

Electro-activation has been observed in the electron transfer process (ETP) of PDS (Chen et al., 2014), and some researchers have suggested that PDS can be adsorbed on the electrode surface in an electrochemical system and then induced to a transient *PDS (Song et al., 2017), while others have insisted that the formation of substantial complexes after PDS adsorption on catalytic materials plays a significant role in triggering the non-radical pathway to degrade pollutants. In this study, nitrogen doping treatment increased the number of polar groups on the surface (Fig. 4) and enhanced the adsorption capacity for sulfur-containing substances such as CH_3SH and H_2S. Polar functional groups such as C=O and pyridinic-N could strengthen the dielectric properties of the carbon materials and facilitate PDS adsorption on the AC surface (Ma et al., 2022), which made it more beneficial for the N-doped AC to participate in the electron transfer process. During S-VOC purification, the conductivity in absorption solution increased owing to continuous PDS conversion and S-VOC decomposition, and the oxidation peaks in the LSV curves increased (Fig. 6), resulting in a moderate increase in the ETP. As a result, the radicals SO_4^{-}• and the other induced highly reactive substances such as HO• and $^1O_2$ were more efficiently activated in 3DES system (Fig. 5).

3.3.4 Pathway of S-VOC purification in 3DES system

Based on the results obtained in this study, a pathway for S-VOC purification in an electrochemical system with N-doped AC is proposed (Fig. 7). As the sulfur-containing inlet gas entered the PDS absorption solution, the amount of S-VOC directly dissolved in the solution was relatively low as most of the S-VOC, such as CS_2 and CH_3SH, are insoluble in water. However, the particle electrode prepared by the N-doped AC had the characteristics of large specific surface area and strong polar functional groups (Figs. 4(b)–4(d), Table 1), which enhanced the adsorption capacity for sulfur-containing substances (Fig. 4(a)), and the targeted components in the inlet gas had a longer residence time in the absorption solution, facilitating the subsequent oxidation decomposition of S-VOC.

In 3DES, those highly reactive substances such as SO_4^{-}•, HO•, and $^1O_2$ were produced as a result of PDS activation (Fig. 5). PDS molecules can be adsorbed on electrode surfaces, resulting in the formation of activated state *PDS (Song et al., 2017). The decomposition of sulfur-containing substances was achieved by radical and non-radical oxidation (Liu et al., 2019; Zheng et al., 2021) according to Eqs. (5)–(8). As the S-VOC purification proceeded, the PDS concentration decreased, and the sulfate ions gradually accumulated in the absorption solution. This was influenced by S-VOC conversion and PDS decomposition, which resulted in sulfate deposition onto the surface of the carbon-based material (Luo et al., 2024) and caused potential adverse effects on S-VOC purification (Figs. 3(c) and 3(d)). However, the conductivity of the absorption solution increased with an increase in sulfate ions, and the oxidation peaks (Fig. 6(d)) and EPR signals of DMPO-•OH and TEMP-$^1O_2$ (Figs. 5(c) and 5(d)) became more pronounced than in the early stage. Thus, radical HO• and non-radical $^1O_2$ contributed more significantly to S-VOC purification (Figs. 5(a) and 5(b)).

The sulfur-containing components in the solution underwent hydrolysis reaction according to Eqs. (8)–(10), and COS was an inevitable intermediate during S-VOC purification (Figs. 1(b), 1(d) and 1(f); Fig. 2(b); Fig. 3(b)), implying that the decomposition of S-VOC, such as CS_2 and CH_3SH, involved multiple reaction steps. The intermediate component, COS, can be further oxidized (Chen et al., 2019; Qu et al., 2022) because the C=S bond is easily broken to form H_2S and CO_2 (Eq. (11)). In the 3DES system with N-doped AC, the adsorption and electrochemical properties significantly

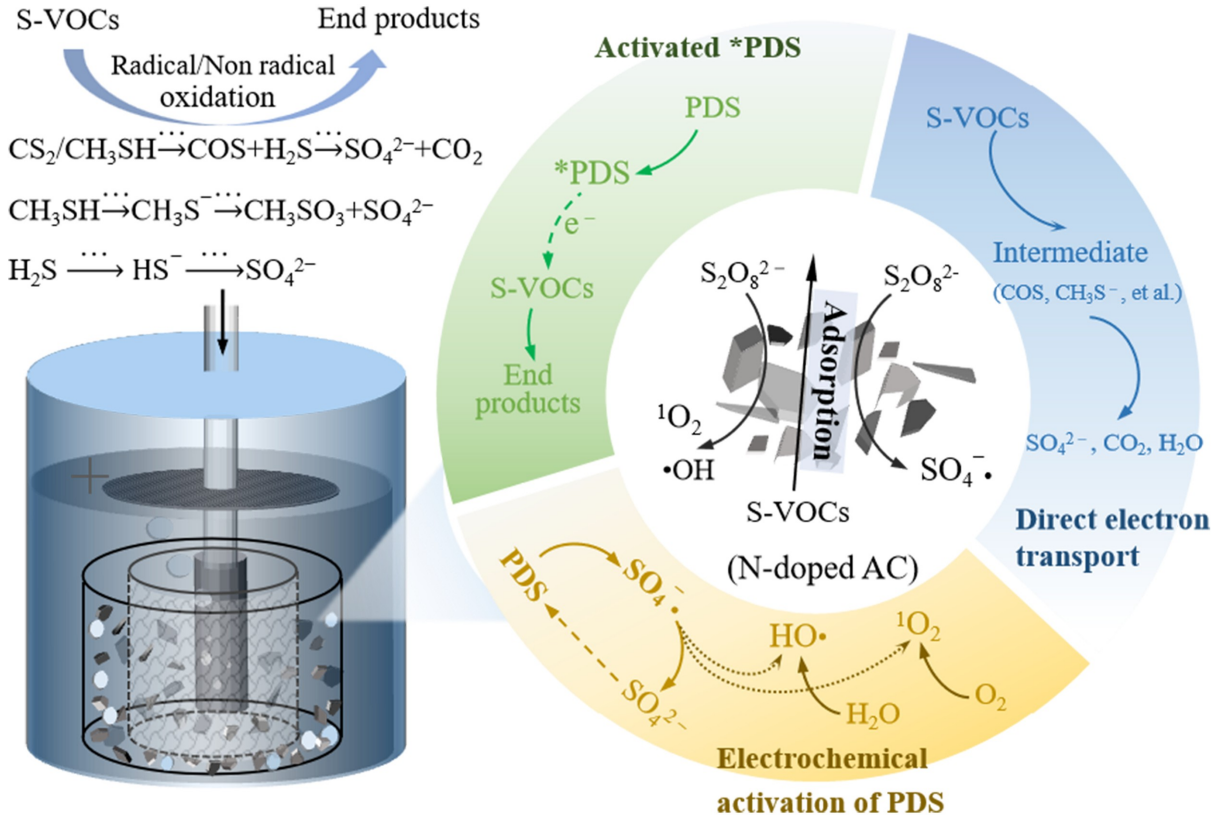

Fig. 7 Proposed pathway of S-VOC oxidation in 3DES process with N-doped AC.

improved, making the oxidative decomposition of the S-VOC more complete. Thus, this 3DES system always maintained a relatively high S-VOC removal, but the H_2S content in the outlet gas was too low to be detected because of the rapid H_2S conversion (Eq. (12)) and the accumulated COS was low throughout the S-VOC purification process.

$$S_2O_8^{2-} + e^- \xrightarrow{AC_{surface}} SO_4^{\cdot-} + SO_4^{2-} \quad (5)$$

$$SO_4^{\cdot-} + OH^- \rightarrow SO_4^{2-} + HO\cdot,\ H_2O \xrightarrow{\text{electrolysis}} HO\cdot + H^+ \quad (6)$$

$$2S_2O_8^{2-} + 4OH^- \rightarrow 4SO_4^{2-} + 2H_2O + {}^1O_2,$$
$$O_2 + e^- \rightarrow O_2^{\cdot-},\ O_2^{\cdot-} + HO\cdot \rightarrow OH^- + {}^1O_2^- \quad (7)$$

$$\text{S-VOC} \xrightarrow[\text{oxidation}]{\text{reactive substances}} \text{Intermediate} + SO_4^{2-} + CO_2$$
$$+ H_2O \rightarrow SO_4^{2-} + CO_2 + H_2O \quad (8)$$

$$CS_2 + H_2O \rightarrow COS + H_2S \quad (9)$$

$$CH_3SH + H_2O\ COS \rightarrow + H_2S, CH_3SH \rightarrow$$
$$CH_3S^- \rightarrow CH_3SO_3 + SO_4^{2-} \quad (10)$$

$$COS + H_2O \rightarrow H_2S + CO_2 \quad (11)$$

$$H_2S \rightarrow HS^- + H^+, HS^- + O_2 \rightarrow SO_4^{2-} + H^+ \quad (12)$$

4 Conclusions

N-doped AC was successfully prepared by modifying raw AC with urea impregnation followed by heat treatment. When employed in the 3DES process, the resulting particle electrode exhibited a large specific surface area and strong polar functional groups, which enhanced its adsorption performance for S-VOC. Thus, the sulfur-containing components in the inlet gas had a longer residence time in the absorbent solution, which facilitated the subsequent oxidative decomposition of S-VOC.

When the simulated S-VOC entered the PDS absorption solution, the purification efficiencies for CH_3SH, H_2S, and NH_3 in the N-doped AC system were approximately 100% under the optimized electrochemical parameters. The CS_2 removal was higher than 90%, the COS content in outlet gas was usually undetectable within 120 min, and the efficacy of S-VOC purification in this electrochemical system was superior to that of the other systems.

In the 3DES process with N-doped AC, PDS was efficiently activated by carbon-based material and electrochemistry. The highly reactive substances, including SO_4^{-}•, HO•, $^1O_2$, and transient *PDS, played significant roles for S-VOC removal, and the complete conversion of sulfur-containing substances was closely related to radical and non-radical oxidations.

Conflict of Interests The authors declare that the research was conducted in the absence of any commercial or financial relationships that could be construed as a potential conflict of interest.

Acknowledgements This work was financially supported by the the Reserve Talents of Young and Middle-aged Academic and Technical Leaders in Yunnan Province, China (No. 202105AC160096).

References

Chen J Y, Chen A G, Qiu P L, Huang L W, Zhou Q H (2019). Removal of carbon disulfide from air stream by absorption combined with electrochemical oxidation. Journal of Environmental Chemical Engineering, 7(3): 103167

Chen W S, Jhou Y C, Huang C P (2014). Mineralization of dinitrotoluenes in industrial wastewater by electro-activated persulfate oxidation. Chemical Engineering Journal, 252: 166–172

Cui Y H, Lv X D, Lei J X, Liu Z Q (2017). Synergistic effect of cathode/peroxymonosulfate/Fe^{3+} on phenol degradation. Electrochimica Acta, 245: 201–210

Ding L, Liang H C, Li X Z (2012). Oxidation of CH_3SH by *in situ* generation of ferrate (VI) in aqueous alkaline solution for odour treatment. Separation and Purification Technology, 91: 117–124

Erlind M, Marco S, Saveria S, Salvatore P, Nicoletta D, Paola B, Mariangela L (2023). Enhanced ORR activity of S- and N-modified non-noble metal-doped carbons with bamboo-like C nanotubes grafted onto their surface. Electrochimica Acta, 464: 142946

Feng Y, Lee P H, Wu D, Shih K (2017). Surface-bound sulfate radical-dominated degradation of 1,4-dioxane by alumina-supported palladium (Pd/Al_2O_3) catalyzed peroxymonosulfate. Water Research, 120: 12–21

Ghosh S, Barg S, Jeong S M, Ostrikov K K (2020). Heteroatom-doped and oxygen-functionalized nanocarbons for high-performance supercapacitors. Advanced Energy Materials, 10(32): 2001239

He D D, Hao H, Chen D K, Liu J P, Yu J, Lu J C, Liu F, Wan G, He S F, Luo Y M (2017). Synthesis and application of rare-earth elements (Gd, Sm, and Nd) doped ceria-based solid solutions for methyl mercaptan catalytic decomposition. Catalysis Today, 281: 559–565

He E Y, Huang G, Fan H L, Yang C, Wang H, Tian Z, Wang L J, Zhao Y R (2019). Macroporous alumina- and titania-based catalyst for carbonyl sulfide hydrolysis at ambient temperature. Fuel, 246: 277–284

Hong J, Jo C (2024). Study on morphology and N-doping effects of carbon cathodes for zinc-ion hybrid supercapacitors. Journal of Power Sources, 594: 234006

Huang Z F, Bao H W, Yao Y Y, Lu W Y, Chen W X (2014). Novel green activation processes and mechanism of peroxymonosulfate based on supported cobalt phthalocyanine catalyst. Applied Catalysis B: Environmental, 154–155: 36–43

Jin H K, An Z Y, Li Q C, Duan Y Q, Zhou Z H, Sun Z K, Duan L (2021). Catalysts of ordered mesoporous alumina with a large pore size for low-temperature hydrolysis of carbonyl sulfide. Energy & Fuels, 35(10): 8895–8908

Jing H L, Yang H T, Yu X H, Hu C Q, Li R X, Li H T (2022). Treatment of organic matter and ammonia nitrogen in wastewater by electrocatalytic oxidation: a review of anode material preparation. Environmental Science. Water Research & Technology, 8(2): 226–248

Li J, Yan J F, Yao G, Zhang Y H, Li X, Lai B (2019). Improving the degradation of atrazine in the three-dimensional (3D) electrochemical process using $CuFe_2O_4$ as both particle electrode and catalyst for persulfate activation. Chemical Engineering Journal, 361: 1317–1332

Li X Y, Wu Y, Zhu W, Xue F Q, Qian Y, Wang C W (2016). Enhanced electrochemical oxidation of synthetic dyeing wastewater using SnO_2-Sb-doped TiO_2-coated granular activated carbon electrodes with high hydroxyl radical yields. Electrochimica Acta, 220: 276–284

Li X, Sun F, Qu Z, Zhu X, Gao J H, Zhao G B, Zhang L Q (2023). Insight into synergistic effects of oxygen and nitrogen dual-dopants in carbon catalysts on selective catalytic reduction of NO_x with NH_3: a combined computational and experimental verification. Chemical Engineering Journal, 454: 140098

Liang C, Huang C, Mohanty N, Kurakalva R M (2008). A rapid spectrophotometric determination of persulfate anion in ISCO. Chemosphere, 73(9): 1540–1543

Liu Z, Ding H J, Zhao C, Wang T, Wang P, Dionysiou D D (2019). Electrochemical activation of peroxymonosulfate with ACF cathode: kinetics, influencing factors, mechanism, and application potential. Water Research, 159: 111–121

Luo R, Liu S G, Li C, Huang X F, Ning P, Tian S L (2024). Synergistic removal of sulphur-containing malodourous gases via peroxydisulfate activation in three-dimensional electrode system. Journal of Environmental Chemical Engineering, 12(2): 112169

Lyu Y C, Liu X M, Liu W Q, Tian Y P, Qin Z (2020). Adsorption/oxidation of ethyl mercaptan on Fe-N-modified active carbon catalyst. Chemical Engineering Journal, 393: 124680

Ma Y H, Wang D, Xu Y, Lin H, Zhang H (2022). Nonradical electron transfer-based peroxydisulfate activation by a Mn-Fe bimetallic oxide derived from spent alkaline battery for the oxidation of bisphenol A. Journal of Hazardous Materials, 436: 129172

Qu J, Wang X Q, Wang L L, Xu B, Ning P, Ma Y X, Xie Y B, Cao

R, Ma Q (2022). The investigation of the role of nitrogen in the improvement of catalytic activity and stability of Zr/Ti-based material for carbon disulfide hydrolysis. Separation and Purification Technology, 296: 121357

Song H R, Yan L X, Ma J, Jiang J, Cai G Q, Zhang W J, Zhang Z X, Zhang J, Yang T (2017). Nonradical oxidation from electrochemical activation of peroxydisulfate at Ti/Pt anode: efficiency mechanism and influencing factors. Water Research, 116: 182–193

Sun H W, He F, Choi W Y (2020). Production of reactive oxygen species by the reaction of periodate and hydroxylamine for rapid removal of organic pollutants and waterborne bacteria. Environmental Science & Technology, 54(10): 6427–6437

Tian R, Lu J C, Xu Z Z, Zhang W J, Liu J P, Wang L L, Xie Y B, Zhao Y T, Cao X H, Luo Y M (2023). Unraveling the synergistic reaction and the deactivation mechanism for the catalytic degradation of double components of sulfur-containing VOCs over ZSM-5-based materials. Environmental Science & Technology, 57(3): 1443–1455

Wang B S, Zhao P Y, Zhang X N, Zhang Y, Liu Y M (2024). Three-dimensional electro-Fenton system with iron-carbon packing as a particle electrode for nitrobenzene wastewater treatment. Frontiers of Environmental Science & Engineering, 18(11): 138

Wang J, Duan X, Gao J, Shen Y, Feng X H, Yu Z J, Tan X Y, Liu S M, Wang S B (2020). Roles of structure defect oxygen groups and heteroatom doping on carbon in nonradical oxidation of water contaminants. Water Research, 185: 116244

Wang Z Q, Huang J C, Wang B, Hu W, Xie D, Liu S, Qiao Y (2022). Co-hydrothermal carbonization of sewage sludge and model compounds of food waste: influence of mutual interaction on nitrogen transformation. Science of the Total Environment, 807(3): 150997

Xiao Q L, Cai S Y, Liu J Z (2021). Microbial and thermogenic hydrogen sulfide in the Qianjiang depression of Qianghan basin: insights from sulfur isotope and volatile organic sulfur compounds measurements. Applied Geochemistry, 126: 104865

Yang J L, Huang Y J, Chen Y W, Xia D H, Mou C Y, Hu L L, Zeng J W, He C, Wong P K, Zhu H Y (2020). Active site-directed tandem catalysis on CuO/VO-MnO_2 for efficient and stable catalytic ozonation of S-VOCs under mild condition. Nano Today, 35: 100944

Yang S Y, Li L, Xiao T, Zheng D, Zhang Y T (2016). Role of surface chemistry in modified ACF (activated carbon fiber)-catalyzed peroxymonosulfate oxidation. Applied Surface Science, 383: 142–150

Yao X L, Wan K, Yu W X, Liu Z (2024). Enhancing comprehension of water vapor on adsorption performance of VOC on porous carbon materials and its application challenge. Frontiers of Environmental Science & Engineering, 18(9): 110

Zhang C, Jiang Y H, Li Y, Hu Z, Zhou L, Zhou M (2013). Three-dimensional electrochemical process for wastewater treatment: a general review. Chemical Engineering Journal, 228: 455–467

Zhao S Z, Yi H H, Tang X L, Kang D J, Gao F Y, Wang J G, Huang Y H, Yang Z (2018). Removal of volatile odorous organic compounds over NiAl mixed oxides at low temperature. Journal of Hazardous Materials, 344: 797–810

Zheng W T, Liu Y B, Liu W, Ji H D, Li F, Shen C S, Fang X F, Li X, Duan X G (2021). A novel electrocatalytic filtration system with carbon nanotube supported nanoscale zerovalent copper toward ultrafast oxidation of organic pollutants. Water Research, 194: 116961

Zhu S S, Huang X C, Ma F, Wang L, Duan X G, Wang S B (2018). Catalytic removal of aqueous contaminants on N-doped graphitic biochars: inherent roles of adsorption and nonradical mechanisms. Environmental Science & Technology, 52(15): 8649–8658